Research Article

Utilization of Rice Husk and Alum Sludge to Produce an Efficient Adsorbent Composite for Recovery of Nutrients from Wastewater

Nguyen Thi Van Anh
International Analysis Center, Ho Chi Minh City University of Industry and Trade, Ho Chi Minh City, Vietnam
Faculty of Environment and Natural Resources, Ho Chi Minh City University of Technology (HCMUT), Ho Chi Minh City, Vietnam
Vietnam National University Ho Chi Minh City, Ho Chi Minh City, Vietnam

Nguyen Ngoc Hoa
Faculty of Chemical Engineering and Technology, Ho Chi Minh City University of Industry and Trade, Ho Chi Minh City, Vietnam

Nguyen Thi Thuy*
School of Chemical and Environmental Engineering, International University, Ho Chi Minh City, Vietnam
Vietnam National University Ho Chi Minh City, Ho Chi Minh City, Vietnam

Nguyen Lan Thanh and Nguyen Nhat Huy*
Faculty of Environment and Natural Resources, Ho Chi Minh City University of Technology (HCMUT), Ho Chi Minh City, Vietnam
Vietnam National University Ho Chi Minh City, Ho Chi Minh City, Vietnam

* Corresponding author. E-mail: ntthuy@hcmiu.edu.vn, nnhuy@hcmut.edu.vn DOI: 10.14416/j.asep.2023.08.002
Received: 16 March 2023; Revised: 2 May 2023; Accepted: 31 May 2023; Published online: 11 August 2023

Abstract
This study focused on developing an adsorbent composite from rice husk and alum sludge to recover nutrients from wastewater, which could be used in the future for slow-release fertilizer production. A biochar-sludge composite (80B/20S) was created by modifying rice husk biochar with $MgCl_2$ and using acid- and heat-treated alum sludge to extract ammonium and phosphate contents from wastewater. The physical and chemical properties of the materials were analyzed using various techniques, such as X-ray diffraction and scanning electron microscopy. In the nutrient recovery test, the contact time, adsorbent dosage, and initial concentration were evaluated. The adsorption equilibrium contact time for both ammonium and phosphate were found to be 8 h, and the maximum adsorption capacity by Langmuir isotherm for the 80B/20S composite was 185.53 mgNH_4^+/g and 63.78 mgPO_4^{3-}/g. The composite material had a higher surface area of 141.32 m^2/g, which promoted its adsorption capacity. Additionally, this material demonstrated a removal efficiency above 85% when applied to actual wastewater. Since the composite is composed mainly of natural components, it has the potential to be used as a sustainable slow-release fertilizer for agricultural growth.

Keywords: Alum sludge, Ammonium, Biochar, Phosphate, Rice husks, Nutrient recovery

1 Introduction

Eutrophication is currently one of the most severe environmental issues affecting water bodies all over the world, thus a reduction in the discharge of nutrients from human activities into the environment and aquatic ecosystems to protect water sources is strongly important. Eutrophic water contains lots of ingredients such as carbon, nitrogen, phosphorus, magnesium, and potassium; however, nitrogen (N) and phosphorus (P) play the most important roles. The rapid population growth and urbanization lead to the discharge of large quantities of nitrogen- and phosphorus-rich wastewater and cause nutrient pollution in the water source. Furthermore, the overuse of pesticides or chemical fertilizers in agriculture significantly increases the release of nitrogen and phosphorus into aquaculture systems. Excessive use of pesticides and chemical fertilizers in agriculture can cause runoff into adjacent water bodies such as rivers, lakes, and seas. When this occurs, the excess nitrogen and phosphorus in these compounds can produce eutrophication, in which an excess of nutrients causes an overgrowth of algae and other plants in bodies of water. Moreover, animal manure and aquaculture feed are also major sources of nutrient pollution in water. Eutrophication reduces water quality in ecosystems, causing biodiversity loss, algal blooms, mass death of fish, and heavy economic losses. The most common methods for resolving water eutrophication are adding chemicals, stimulating aquatic plant metabolism, and aerating/diluting wastewater/water [1]. However, these approaches may generate secondary pollution, necessitate extreme conditions, or be prohibitively expensive [1]. As a result, a new, cost-effective, and environmentally sustainable approach to nutrient recovery in the aquatic ecosystem is crucial.

Biochar is an efficient and environmental-friendly adsorbent for solving water pollution problems and shows enormous potential for use in removing inorganic nutrients from wastewater. Biochar could be produced through the biomass pyrolysis process [1]. Biochar has various adsorption pathways for NH_4^+, and PO_4^{3-}. Cation exchange capacity (CEC), acid functional groups, and the electrostatic interaction of NH_4^+ with oxygen-containing functional groups on the surface all influence NH_4^+ adsorption, while PO_4^{3-} adsorption is mainly related to the nanocomposite structure or crystals of metal oxides on the surface [2], [3]. The modification of biochar involves the addition/generation of functional groups containing oxygen or nitrogen onto its surface, as well as the incorporation of metal oxides. Several studies have shown that biochar containing metal oxides (e.g., CaO, MgO, Fe_2O_3, Al_2O_3, and La_2O_3) exhibits higher N and P adsorption capacity than raw biochar. Furthermore, the metal oxide layer formation on the surface also significantly increases the surface area and the pore structure that is conducive to the physical adsorption mechanism, thereby improving the N and P adsorption capacity of biochar [4]–[7].

In some studies, Mg is the metal combined with biochar to enhance the NH_4^+ and PO_4^{3-} adsorption efficiency. The addition of MgO with a content of 8.3% to 26.1% increases the adsorption capacity of PO_4^{3-}, which is thought to be caused by positively charged MgO precipitating on the surface [8]. In another study [4], phosphate adsorption potential in water was enhanced by Mg-biochar composites, with statistical analysis showing a clear correlation ($R^2 = 0.78$ and $p < 0.001$) between the P removal rate and the Mg content in the biochar. Mg in biochar will cause a lot of colloidal or nano oxide particles to form on the carbon surface, which can adsorb P through electrostatic attraction to form complexes that are deposited on the surface [4]. Furthermore, the study of He *et al.*, demonstrates the presence of N-containing organic matter on the surface of the biochar, a binding energy peak at 398.50 eV was observed following the addition of Mg content in biochar, which was associated with the C-N bond. It is plausible that the adsorption of NH_4^+ occurred on the surface of the biochar through either negatively charged surface functional groups or cation exchange [9]. Also, the research of Xiao *et al.*, displayed the rise of Mg^{2+} leading to an increase in NH_4^+ adsorption capacity [10]. With a maximum adsorption capacity of 398 mg/g and 22 mg/g, respectively, the biochar mixture impregnated with $MgCl_2$ 20% followed by carbonization demonstrated a good preference for phosphate and ammonium removal [11]. Pyrolysis oak and corncob at 550 °C and 350 °C were used to compare the removal efficiency of NH_4^+ and PO_4^{3-} before and after washing with deionized water, showing that washing after pyrolysis lost some metal content on the surface of the material and lead to a reduction in phosphate removal efficiency

by 25–100% compared to biochar that has not been washed [12]. Sugar beet waste that slowly pyrolyzed at 600 °C gave a removal efficiency of more than 73% of PO_4^{3-} because of the existence of nano-sized MgO colloids on the exterior of the material [4], [13]. Many different types of biomass were examined, and the results revealed that MgO-biochar nanocomposite from beet and peanut pods had the highest phosphate adsorption capacity of 835 mg/g [5]. MgO nanoparticles had high crystallinity and were evenly deposited on the entire surface of biochar, thus this physical and chemical properties lead to a high capacity for phosphate adsorption [5], [14].

As an agricultural country, the fields of rice are an important utilization of land in Vietnam, which comprises around 14% (42,500 km^2) of the entire land area [15]. In Vietnam, it is estimated that approximately 39 million tons of rice residue are produced annually, with each hectare of rice generating approximately 5 tons of wastes [16]. Typically, rice farming by-products like straw and husks have been utilized as fuel and fertilizer. Yet in Vietnam and other Asian countries, crop wastes are being burned in the field after harvesting [16]. In the research of Duong and Yoshiro [17], Vietnamese farmers frequently burn rice straw after harvesting, with a large rate of 70–80% in the northern area and more than 90% in the southern region. As reported by Truc *et al.* [18], roughly 10% of them were left on the land. Based on a 2011 study in Can Tho, 60% of rice straw or husk was burnt and 40% was absorbed into the soil [19]. Moreover, about 20 kg of husks from 100 kg of paddy fields are disposed or burnt every years [20]. On the other hand, carbon monoxide (CO), carbon dioxide (CO_2), methane (CH_4), nitrous oxide (N_2O), nitrogen oxides (NO_x), and sulfur dioxide (SO_2) are all released when agricultural wastes are burned on the field. Rice husk is a common agricultural by-product in developing countries like Vietnam, but little research has been done on using it as an adsorbent for the recovery of N and P in wastewater. Therefore, this will be a new research direction, which is highly practical in terms of both environmental treatment and agriculture development. Because of its high volatile matter content (70.2–78.5%) and carbon content (35.2–44.7%), pyrolysis was discovered to be advantageous for creating biochar from rice husks [21]. In some works, rice husk was modified to adsorb ammonium from piggery manure anaerobic digestate with an adsorption capacity of 39.8 mg/g [22]. Furthermore, rice husk biochar can be used for removing emerging compounds like azithromycin and erythromycin (about 95% of inlet concentration 200 mg/L) [23]. And, rice husk biochar activates with NaOH can remove about 72% cadmium with a capacity of 17.8 mg/g [24]. From the literature above, rice husk would be utilized as an adsorbent for contaminants removal. The adsorption capacity of ammonium ion with various types of biomass, such as mixed wood at 54.86 mgN/g, rice husk at 47.14 mgN/g, and municipal waste at 137.3 mgN/g was found [25].

Alum sludge is a popular solid waste from water supply and wastewater treatment. Using sludge as an adsorbent for pollutants is considered a potential alternative [26]. The characteristics of the sludge depend on the water source and treatment technology. Normally, alum sludge consists of organic compounds, macronutrients, micronutrients, metals, organic microbiological contaminants, and microorganisms. Utilizing industrial and agricultural wastes to create an environmental-friendly and low-cost material capable of handling organic pollutants in the water is a direction worth considering. In particular, previous studies showed that alum sludge has a potential adsorption capability and can be used in wastewater treatment as a "low-cost" phosphorus adsorbent [27], [28]. This is attributed to the metal ions in the alum sludge, which improves the process of adsorption and chemical precipitation that help to remove pollutants from wastewater [29], [30]. In Vietnam, river water is the primary source of water, where all the large water supply treatment plants use coagulation with alum (e.g., aluminum sulfate, polyaluminum chloride, and iron sulfate) to treat the raw water and the alum sludge are produced daily with a huge amount. This source of alum sludge is relatively "clean" with the natural composition of river water (e.g., colloids, natural organic matters, microorganisms, clays, and silica) and metals (e.g., Ca from limestone and Al from polyaluminum chloride). However, it is still classified as industrial solid waste and sometimes hazardous waste in Vietnam because it is "sludge" from water/wastewater treatment. Therefore, water treatment plants spent a lot of money to handle this waste and its utilization is very limited. There are a plethora of related research exploring the adsorption capabilities of different types of biomasses, such as sewage

sludge ash and willow of Konczak *et al.* [31], and Mg-phosphorus rich biochar of He *et al.* [32], $MgCl_2$-phosphate based australis biochar of Jiang and Konczak *et al.* [31], [33], or municipal waste and greenhouse waste with heat treatment for ammonium removal [34].

Given the nature of MgO-rice husk and alum sludge, combining these two wastes to produce a composite that can be utilized as an efficient adsorbent for ammonium and phosphate recovery in wastewater is an excellent concept. Unfortunately, there has been no mention of this topic that can be seen in the literature yet. A unique strategy that has recently attracted interest in the scientific community is the use of sludge and rice husk as charcoal adsorbents for nitrogen removal from wastewater. This technique has various benefits over conventional adsorbents, including low production costs and ample raw material availability. The use of sludge and rice husk biochar also tackles waste disposal issues and provides a long-term solution for wastewater treatment at low cost. Moreover, this biochar's adsorption capability is equivalent to that of other regularly used adsorbents. For the current situation in Vietnam, the eutrophication, rice husk in land field and the alum sludge from water treatment plant, we come up with this research about combining rice husk and alum sludge as an adsorbent for recovery ammonium and phosphate from domestic wastewater. This study can produce a low-cost but high-efficiency adsorbent using agricultural and industrial wastes as an alternative method to recover nutrients from wastewater. This method can be applied to large-scale production and is suitable for developing countries. Additionally, the study aims to reduce waste entering the environment by taking advantage of sludge and to reduce costs associated with treatment, transportation, and landfilling. As a result, this study provides a novel and promising technique for efficient nutrient removal from wastewater. Finally, the nutrient-rich biochar-sludge composite produced after adsorption can serve as a source of slow-release fertilizers for agricultural activities.

2 Materials and Methods

2.1 *Material preparation and characterization*

Rice husk was collected at a rice milling factory in Thoi Lai District, Can Tho City, Vietnam. After cutting into small pieces with a size of < 2 mm, it is washed with deionized water to dissolve dust particles, and then overnight in an oven at 80 °C. Salt of $MgCl_2.6H_2O$ was used to prepare 4% (w/w) $MgCl_2$ solution. The pretreated rice husk was impregnated with the prepared $MgCl_2$ solution at a ratio of 1 g per 20 mL. The suspension was stirred at a speed of 300 rpm for 24 h at room temperature and then dried at 105 ℃ for 6 h in an oven. After that, the impregnated rice husk was pyrolyzed at 500 ℃ for 15 min at a heating rate of 10 ℃/min. The collected biochar was crushed into a powder with a particle size of < 0.2 mm.

Alum sludge was collected at the Tan Hiep Water Treatment Plant in Hoc Mon District, Ho Chi Minh City, Vietnam. The sludge was crushed into powder with a size of about 0.2–0.45 mm and dried at 80 ℃ in an oven overnight. The pretreated alum sludge was then heated at 500 ℃ for 1 h at a heating rate of 10 ℃/min. After that, 5 g of the heat-treated sludge was activated with 0.1 N H_2SO_4 solution. Finally, the modified biochar was mixed with the activated alum sludge at different ratios to form the adsorbent composites, which were used to remove ammonium and phosphate in the solution.

X-ray diffraction was used to investigate the mineral composition and crystal phase of the samples (XRD; D2 Phaser, Bruker, Germany) with Cu tube 1.5484 Å, Lynxeye (1D mode) detector. Scanning electron microscopy (SEM; JSM-IT200, JEOL, Japan) and energy-dispersive X-ray spectroscopy (EDX) were used to determine the material's morphology and elemental composition. The gas adsorption approach was used to determine the surface area and pore size distribution of the materials using a Brunauer–Emmett–Teller (BET) study of the N_2 gas isotherm adsorption curve at –196 °C (Surfer, Thermo Scientific, USA). The surface chemistry and functional groups of the materials were determined using Fourier-transform infrared spectroscopy (FTIR) (Tensor 27, Bruker, Germany).

2.2 *Batch adsorption experiments*

2.2.1. Adsorption of ammonium and phosphate

A solution that contains a mixture of ammonium (50 mgNH_4^+/L) and phosphate (50 mgPO_4^{3-}/L) was

prepared using KH_2PO_4 and NH_4Cl, which were diluted to the required concentration. For each batch adsorption experiment, 0.1 g of adsorbent was poured into a Beaker of 100 mL of the specified ammonium and phosphate concentration solution. A magnetic stirrer was used to stir the mixture at 300 rpm under room temperature for 12 h. The samples were taken and purified immediately after adsorption through 0.45 mm membranes to isolate the adsorbent from the ammonium and phosphate solution. The solution was then analyzed for obtaining the concentrations of ammonium and phosphate. Ammonium concentration was analyzed using the automatic titration distillation method (FOSS, Sweden) while phosphate was stained with the reagent and measured with an ultraviolet-visible spectrophotometer (UV-Vis, 6705 Jenway, England).

The following Equations (1) and (2) were used to measure the removal efficiency (H, %) and adsorption capacity (Q, mg/g):

$$H = \left(1 - \frac{C_t}{C_o}\right) \times 100\% \quad (1)$$

$$Q = \frac{(C_o - C_t) \times V}{m} \quad (2)$$

Where C_o and C_t (mg/L) are the concentrations of ammonium or phosphate at the beginning and after a certain time. V (L) is the volume of the solution and m (g) is the amount of the adsorbent.

2.2.2. Kinetic models

The pseudo-first-order kinetic model was given in Equation (3) [35]:

$$\ln(Q_e - Q_t) = \ln Q_e - k_1 t \quad (3)$$

The pseudo-second-order kinetic model was given in Equation (4) [35]:

$$\frac{t}{Q_t} = \frac{1}{k_2 Q_e^2} + \frac{t}{Q_e} \quad (4)$$

Intra-particle diffusion model was given in Equation (5) [36]:

$$Q_t = k_{ip} t^{0.5} \quad (5)$$

Where k_1, k_2, and k_{ip} are the equilibrium rate constant of the pseudo-first-order equation (1/min), the pseudo-second-order rate constant (g/(mg.min)), and the intra-particle diffusion rate constant (mg/(min$^{1/2}$.g)), respectively. C is a constant, which is the intercept of the intra-particle diffusion equation, and t is the contact time (min). The parameter Q_t is the adsorption amount at a certain time t (mg/g), and Q_e is the adsorbed amount at equilibrium (mg/g) [37].

2.2.3. Isotherm models

According to the Langmuir model, it is assumed that the molecules only adsorb to form a monolayer on the surface of the material without any interactions between adsorbing molecules, as shown in Equation (6):

$$\frac{C_e}{Q_e} = \frac{1}{K_L Q_{max}} + \frac{C_e}{Q_{max}} \quad (6)$$

The Freundlich model is used to describe adsorption processes on heterogeneous surfaces, and it is used to calculate surface heterogeneity and the exponential distribution of active positions and energy, which is expressed in Equation (7):

$$\ln Q_e = \ln K_F + \frac{1}{n} \ln C_e \quad (7)$$

Where Q_e is the adsorbed amount of ammonium or phosphate on the adsorbent at the equilibrium concentration of adsorbate in solution (mg/g) and C_e denotes the concentration of ammonium or phosphate at equilibrium (mg/L). K_L (L/mg) and K_F ((mg/g).(L/mg)$^{1/n}$) are the Langmuir and Freundlich constants, respectively. Q_{max} is the maximum adsorption capacity (mg/g) and the parameter n is the Freundlich exponent related to the intensity of adsorption. [36], [37].

3 Results

3.1 *Ammonium and phosphate adsorption by different materials*

MgO impregnation had a significant impact on biochar adsorption efficiency, as exhibited in Figure 1. When the $MgCl_2$ content increased, the ammonium treatment efficiency increased significantly and reached over 90% (equivalent to an adsorption capacity of above 60 mgNH_4^+/g) at an $MgCl_2$ content of ≥ 3%.

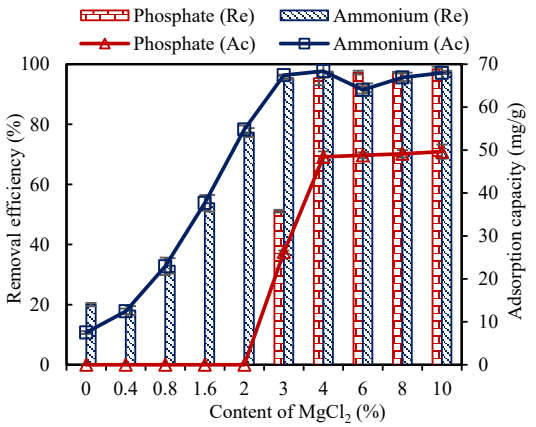

Figure 1: The influence of $MgCl_2$ content on biochar adsorption capability.

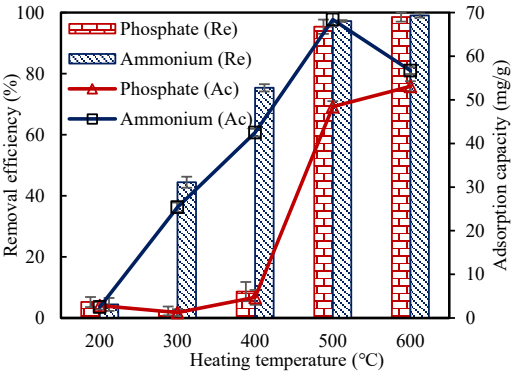

Figure 2: Effect of carbonization temperature on adsorption ability of MgO-modified biochar with adsorbate removal efficiency (Re, %) and adsorption capacity (Ac, mg/g).

In addition, phosphate was almost not removed from the solution with materials having $MgCl_2$ content less than 3%. With an $MgCl_2$ content of ≥ 3%, the phosphate removal efficiency improved significantly. At the content of 4%, both ammonium and phosphate were treated with quite high efficiencies of 97.24 ± 0.29% and 95.36 ± 2.36%, respectively, which were equivalent to adsorption capacities of 68.38 ± 1.51 mgNH_4^+/g and 48.43 ± 1.27 mgPO_4^{3-}/g. Compared to non-modified biochar, the modified one containing two solid phases, scilicet nano-crystals of metal oxides and biochar matrix, exhibits enhanced adsorption ability for a wide range of contaminants [21]. These phases contributed to the adsorption capacity via various mechanisms, including precipitation, hydrogen bonding, ligand exchange, and electrostatic precipitation [21].

The enhanced phosphate removal by MgO impregnation was likely due to the formation of nanoscale MgO particles dispersed on the biochar surface. The enhancement of phosphate adsorption with MgO was the weak bonds between them (surface deposition through hydrogen bond), or precipitation by strong chemical bond [38]. During the pyrolysis process, Mg oxide undergoes a continuous cycle of forming and breaking the C-O-Mg bond. This results in the movement of Mg^{2+} ions from the interior of biochar to its surface. This movement, as reported by Zhu *et al.* [39] enhanced the concentration of active components in biochar and increased the potential for volatile production. Furthermore, at high temperatures, the unstable Mg^{2+} ions convert to MgO and remain stable on the surface of the biochar [9]. Additionally, dissolved MgO in solution may cause chemical reactions between Mg^{2+} and PO_4^{3-}, resulting in $Mg_3(PO_4)_2$ or $MgHPO_4$ precipitates. Also, after being modified with MgO, the formed porous structures of biochar were very useful in removing phosphate and ammonium from the solution [5]. MgO particles would combine with NH_4^+ and PO_4^{3-} ions to produce a precipitate of struvite ($NH_4MgPO_4.6H_2O$). For ammonium ion adsorption, Mg^{2+} was similarly the dominating cation exchanger [40]. Struvite is a slow-release fertilizer containing nutritional values of N and P that can be applied to the soil and used as a slow-release fertilizer for agriculture crops. For phosphate and ammonium adsorption, the size distribution and morphological structure of MgO particles in biochar structure are important. According to these experimental results, the $MgCl_2$ content of 4% was effective for the MgO-modified biochar in removing both ammonium and phosphate and at the same time saving the amount of chemicals needed.

Figure 2 shows the effect of carbonization temperature on the adsorption efficiency of modified biochar. At temperatures below 500 °C, the material had almost no ability to remove phosphate with an efficiency of less than 10%. This is because the organic components in the material were not completely removed, thus the surface area of the

material was not sufficiently large for removing phosphates by physical adsorption mechanism. Regarding ammonium removal, the ammonium adsorption efficiency increased gradually with the carbonization temperature from 200–400 ℃ and the treatment efficiency was over 70% at 400 ℃. However, at temperatures of ≥ 500 ℃, both ammonium and phosphate achieved high adsorption efficiencies of >97 % and >95 %, respectively, and high adsorption capacities of 68.38 ± 1.51 mgNH_4^+/g and 48.43 ± 1.27 mgPO_4^{3-}/g. At 600 ℃, a gradual decrease in ammonium capacity and a negligible increase in phosphate adsorption capacity were observed. This was explained by the beginning of structural damage of the material when carbonized at too high temperatures. The carbonization temperature affects functional groups such as hydroxyl and carboxyl are present, which correlate with ammonium and phosphate removal efficiency via providing cation and anion exchange locations for NH_4^+ and PO_4^{3-} removal. Because of the hydrogen ionization in the solution, the acidic functional groups are negatively charged and the positively charged NH_4^+ is electrostatically attracted and exchanged with H+ [12], [41]. The addition of an acidic functional group helped a lot in promoting the adsorption of ammonium ions [25]. High temperature also increased the evaporation of organic compounds, creating more porous structures, leading to increased surface area for the material and contributing to the increase in the phosphate adsorption efficiency according to the physical mechanism. However, the pore structures tended to change from micropores and mesopores to macropores at too high temperatures (e.g., 600 ℃) and the material gradually transforms to partial ash, leading to no further increase in the adsorption efficiency of the material. Therefore, 500 ℃ was the optimal temperature for carbonizing rice husk and was chosen for further investigation.

The effectiveness of acid type on the performance of activated alum sludge is exhibited in Figure 3. One can see that the acid activation strongly affected the adsorption of phosphate, which depended on different types of acid. Phosphoric acid had almost no effect on sludge activation where the adsorption capacities were very low at only 2.86 ± 1.08 mgNH_4^+/g and 3.32 ± 2.09 mgPO_4^{3-}/g. Meanwhile, sulfuric acid showed a quite high sludge activation ability with a superior phosphate treatment efficiency of 78.13 ± 2.22% (i.e., 83.59 ± 1.84 mgPO_4^{3-}/g) as compared to other acids. However, the sludge activated by acids had almost no effect on ammonium adsorption ability with removal efficiency from 6.15–14.48%. As a result, rice husk biochar was mixed with alum sludge activated with H_2SO_4 for simultaneous ammonium and phosphate recovery in wastewater.

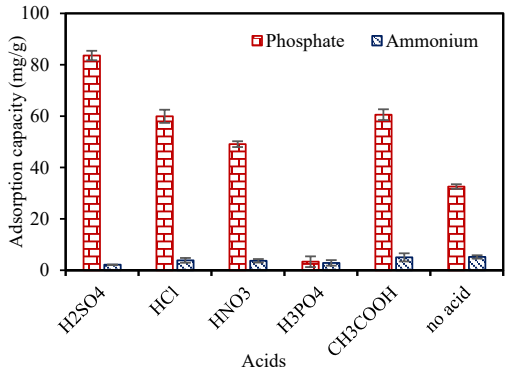

Figure 3: Effect of acid activation on the performance of alum sludge.

As discussed above, the MgO-modified biochar seemed to prefer ammonium adsorption to phosphate, where the phosphate treatment efficiency increased after the ammonium adsorption reached equilibrium. Meanwhile, it could be found that the sludge material was almost exclusively for phosphate treatment. Therefore, to be able to treat both ammonium and phosphates at the same time, it is necessary to investigate the feasible mixing ratio between the modified biochar and activated sludge. The adsorption capacity of ammonium and phosphates of biochar and sludge differs, as shown in Figure 4, and the higher the sludge content in the mixture, the lower the adsorption capacity. The mixing ratio of 80% biochar and 20% sludge (80B/20S) provided the highest adsorption capacity of ammonium and phosphate (i.e., 68.95 ± 1.54 mgNH_4^+/g and 42.42 ± 3.11 mgPO_4^{3-}/g), thus it was chosen as the best composite for further investigation.

3.2 *Effect of environmental factor on the adsorption performance of biochar-sludge composite*

The porous structure, laden active elements, surface groups, and mineral components of biochar all have an impact on its adsorption performance. According to Dai and co-workers, the mechanism of adsorption

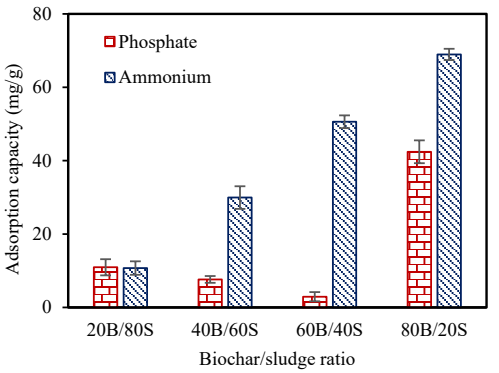

Figure 4: Effect of biochar/sludge ratio on the adsorption of ammonia and phosphate.

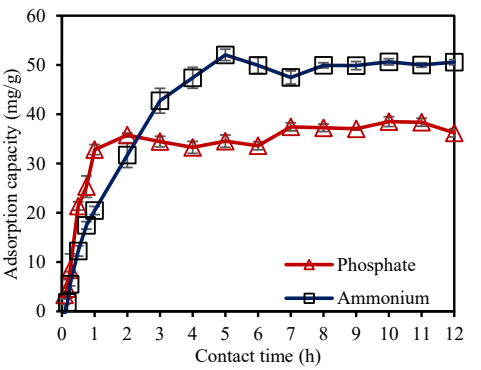

Figure 5: Effect of contact time on adsorption capacity of 80B/20S composite.

is an intricate procedure that incorporates numerous interactions such as electrostatic attraction, surface, complexation, ion exchange, physical adsorption, and precipitation [42], [43]. Therefore, we must conduct several experiments with various factor for evaluating the adsorption mechanism of biochar. The contact time between the adsorbent and the solution is critical when measuring ammonium and phosphate removal performance. Figure 5 shows the influence of exposure time on the ammonium and phosphate adsorption potential of the 80B/20S composite. The adsorption potential of both ammonium and phosphate ions increased with the contact time, with phosphate having a faster time to equilibrium than ammonium. Furthermore, the phosphate's adsorption capacity increased rapidly in the first 2 h, after which it changed slightly but not significantly. Meanwhile, ammonium adsorption capacity increased gradually during the first 8 h of the experiment, when it almost reached equilibrium concentration. When the contact time was extended to 12 h, the adsorption capacities of both ions changed slightly and reached a steady level of about 50 mgNH_4^+/g and 38 mgPO_4^{3-}/g. The rapid equilibrium of phosphate adsorption capacity can be attributed to the chemical reaction between the PO_4^{3-} and the MgO particles on the surface of the material. This reaction occurs rapidly and forms complexes between Mg and PO_4^{3-}, leading to a rapid change in phosphate concentration. On the other hand, there were active centers on the surface of the material containing negatively charged functional groups, which can interact strongly with NH_4^+ ions and captured these ions. As the research of Liu *et al.*, these functional groups were the key elements of NH_4^+ adsorption based on the ion exchange mechanism [6], [44]. Moreover, the study of Wang *et al.*, showed that the amount of acidic functional group was in direct proportion with the adsorption capacity of ammonium ion [6]. Once biochar adsorbents have been engaged for a certain period, their active sites become mostly settled. As a result, the concentration of nutrients in the water inlet drops, driving it more problematic for them to come into reference with the active sites of the adsorbents [43]. When the material was no longer able to capture ammonium and phosphate ions, it became saturated. Thus, the time to reach the adsorption equilibrium of phosphate was 7 h and ammonium was 8 h. Due to the study being carried out to remove both ammonium and phosphate at the same time, 8 h was chosen as the time that reached equilibrium to ensure equilibrium adsorption for both ammonium and phosphate.

The initial ammonium and phosphate concentrations in the solution had a major effect on the material's removal efficiency and adsorption ability. As shown in Figure 6, the adsorption capacities of ammonium and phosphate are proportional to their initial concentrations. Under the higher concentrations of ammonium and phosphate ions, these ions became denser, facilitating the interaction between these ions with the adsorbent, promoting contact and ionic capture of the composite material. This was seen in the concentration range of 10–500 mg/L, where the ammonium adsorption potential began to increase at 9.23 ± 0.54 mg/g and peaked at 126.28 ± 2.22 mg/g at a concentration of 150 mg/L. Meanwhile, phosphate adsorption potential increased from 8.37 ±

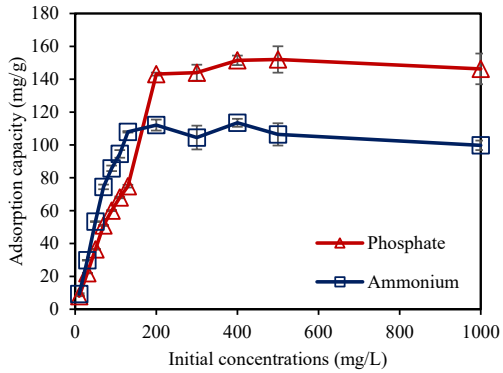

Figure 6: Effect of initial concentration of ammonium and phosphate on adsorption capacity.

0.08 mg/g at a concentration of 10 mg/L to 152.02 ± 8.03 mg/g at a concentration of 500 mg/L. According to the research of Wang *et al.*, the growth in phosphate initial concentration led to the same trend with the adsorption capacity [45]. Changes in phosphorus species could potentially be caused by the effect of phosphate concentration on pH. With the reduction of the phosphate concentration, the amount of ionized H^+ in the water also changes. As a result, hydroxyl protonation or deprotonation may occur on the biochar surface, which can influence the electrostatic attraction of the biochar surface and phosphorous species [42]. The study found that when the initial concentration of ammonium increased, the adsorption capacity of the biochar-sludge composite grew until it reached a saturation point. The amount of nutrients that can be adsorbed by an adsorbent enhances with growth initial concentration, until the adsorption capacity becomes saturated, where further increase in the initial concentration does not result in a rise in the amount of contaminant adsorbed. From the results, the initial concentration of ammonium and phosphate after 200 mg/L was reach the equilibrium stage.

The mass of the adsorbent, in addition to contact time and initial concentration, is one of the factors that govern the effectiveness of ammonium and phosphate adsorptions. This experiment was arranged with different adsorbent dosages from 0.5 to 2 g/L. As shown in Figure 7, the adsorption capacities of ammonium and phosphate were greatly influenced and inversely proportional to adsorbent dosage, i.e., the capacity decreased when increasing dosage. The adsorption capacity is calculated by mg of the

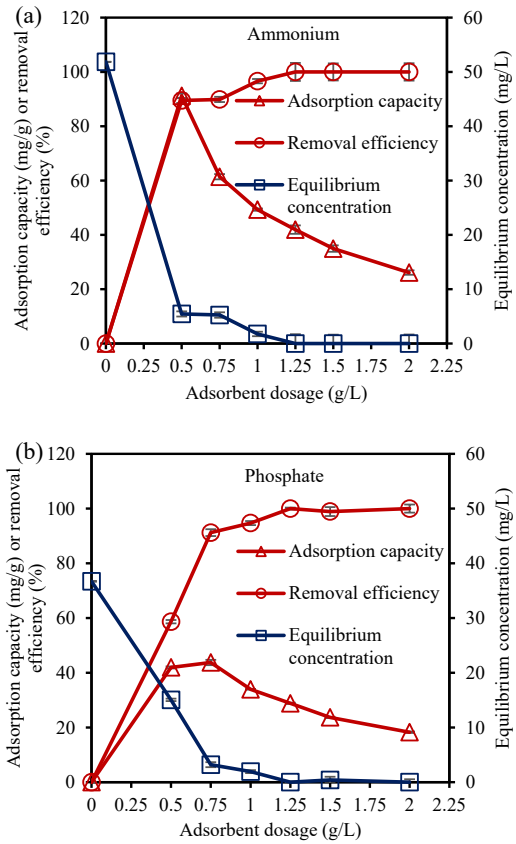

Figure 7: Effect of adsorbent dosage on (a) ammonium and (b) phosphate adsorption performance.

adsorbate per g of the adsorbent. Therefore, when the amount of the adsorbent increases, the initial amount of ammonium and phosphate ions in the solution remains unchanged, leading to a reduction in the potential of adsorption. In addition, when the mass of the material increased, the efficiency of removing ammonium and phosphate also rose because there were more surface and active sites for the adsorption [42]. When using 0.5 g of adsorbent, the removal efficiency reaches 89.50% of ammonium. With the increase of adsorbent, the removal efficiency has just slightly risen in a control value and ammonium was completely removed at 1.25 g material. For the benefit in finance, 0.5 g of adsorbent should be chosen for the optimum value. On the other hand, the removal efficiency of phosphate was 91.21% at 0.75 g/L; thus, it had the same situation as ammonium with completely removed 100% for phosphate. Once biochar adsorbents have

been engaged for a certain period, their active sites become mostly settled. As a result, the concentration of nutrients in the water inlet drops, driving it more problematic for them to come into reference with the active sites of the adsorbents [43].

The Langmuir and Freundlich isotherm models were used to explain the relationship between ammonium and phosphate ion concentrations on the material's surface and their concentrations in the solution at equilibrium under constant temperature conditions in this analysis. From the values of slope and intercept, the parameters of the isotherm equations were obtained and summarized in Table 1. It was found that Langmuir isotherms for both ammonium and phosphate had very high correlation coefficients of $R^2 > 0.98$. However, Freundlich had a lower correlation coefficient than Langmuir for both ammonium and phosphate (i.e., 0.8587 and 0.8258, respectively). As a result, it was thought that the Langmuir isotherm was better for ammonium and phosphate adsorption than the Freundlich isotherm. This proved that the adsorbent had a high homogeneity and the same affinity for ammonium and phosphate ions at all points, and only interacted with a single ion without any significant interaction between them, creating a monolayer bond on the surface of 80B/20S composite. Compared with the research of He *et al.*, the maximum adsorption capacity of ammonium ion and phosphate ion was 37.72 mg N-NH_4^+/g, and 73.28 mg P-PO_4^{3-}/g, respectively [9]. The maximum adsorption capacity of eupatorium adenophorum biochar EBC for phosphate and ammonium removal was 2.32 mg P-PO_4^{3-}/g and 1.909 mg N-NH_4^+/g [46].

The linear equations of the kinetic models are presented in Table 2. Among the three models, the pseudo-second-order model best described the adsorption process with a greater correlation coefficient than the others (e.g., $R^2 = 0.9808$ for ammonium and $R^2 = 0.9875$ for phosphate). Moreover, the adsorption capacities (Q_e) of ammonium and phosphate calculated according to the pseudo-second-order model were the closest to the experimental values while this result for the first-order kinetic model was largely different. Therefore, the adsorption kinetics of ammonium and phosphate in solution following the pseudo-second-order model was the most appropriate one in this study. From the pseudo-second-order model, the adsorption rate constant for the ammonium ion at the concentration of 50 mg/L was calculated to be $K = 8.32 \times 10^{-5}$ (g/mg.min) and the rate constant of phosphate adsorption at a concentration of 50 mg/L was $K = 1.36.10^{-3}$ (g/mg.min). Compared with the research of Cheng *et al.*, the pseudo-second-order kinetic constants were 1.584 gP/mg.min and 3.398 gN/mg.min [46].

Table 1: Isotherm parameters for phosphate and ammonium adsorption on 80B/20S composite

Ammonium	Langmuir	Q_{max} (mg/g)	185.5288
		K_L (L/mg)	0.1496
		R^2	0.9864
	Freundlich	K_f ((mg/g)(L/mg)n)	25.3584
		n	1.9829
		R^2	0.8587
Phosphate	Langmuir	Q_{max} (mg/g)	63.7755
		K_L (L/mg)	5.0580
		R^2	0.9971
	Freundlich	K_f ((mg/g)(L/mg)^n)	38.5374
		n	3.4335
		R^2	0.8258

Table 2: Linear kinetic equations for phosphate and ammonium adsorption using 80B/20S composite

	Parameters	**Kinetic Equation**	Q_e	R^2
Ammonium	Experimental results		49.92	-
	Pseudo-first-order model	$y = –0.0186x + 4.5855$	98.05	0.8854
	Pseudo-second-order model	$y = 0.0133x + 2.1269$	75.19	0.9808
	Intra-particle diffusion model	$y = 3.1062x – 3.7858$	-	0.9697
Phosphate	Experimental results		37.25	-
	Pseudo-first-order model	$y = –0.0048x + 2.4069$	11.10	0.3952
	Pseudo-second-order model	$y = 0.0273x + 0.5742$	36.63	0.9875
	Intra-particle diffusion model	$y = 1.2351x + 15.121$	-	0.5579

The actual domestic wastewater samples were taken for testing the ammonium and phosphate adsorption ability of the 80B/20S composite. Two locations in Ho Chi Minh City (Vietnam) for wastewater sampling included (i) a university dormitory in Tan Phu District (WW1) and (ii) a residential area in Tan Binh District (WW2). As displayed in Table 3, both domestic wastewater samples had ammonium and phosphate concentrations quite consistent with the concentration range investigated in the laboratory. Ammonium and phosphate removal efficiency in actual domestic wastewater was quite high at over 85%. From this result, it can be confirmed that the 80B/20S composite in this study can be completely suitable for ammonium and phosphate removal in domestic wastewater, in line with the research objective of nutrient recovery in wastewater. Besides, the 80B/20S material also showed high selectivity for ammonium and phosphate ions compared to other pollutants in domestic wastewater.

Previous research on the removal of ammonium and phosphate from domestic wastewater has also been performed. The sorption potential of the polymer hydrogel material was 8.8–32.2 mg NH_4–N/g, leading to removal efficiencies ranging from 68 to 80 percent, in order to extract ammonium from domestic wastewater [47]. MgO and dolomite materials heated at different temperatures were used to remove ammonium and phosphate from synthetic wastewater and results showed that ammonium removal was modified with MgO (57%), dolomite 650 °C, and dolomite 750 °C (75%) while the phosphate removal efficiency of these materials was 60% [48]. In a real effluent with a phosphate content of 1.1 mgP/L, $La(OH)_3/Fe_3O_4$(4:1) material with a dosage of 0.1 g/L efficiently reduced the phosphate concentrations to a minimum (0.05 mgP/L with an efficiency of >95%) [49]. Thus, compared with other studies, the 80B/20S material was capable of handling ammonium and phosphate quite well. In Vietnam, the concentrations of ammonium and phosphate in the domestic wastewater output were in line with the discharge standard (e.g., QCVN 14: 2008/BTNMT, National technical regulation on domestic wastewater) into the environment (e.g, < 5 mg/L, Column A).

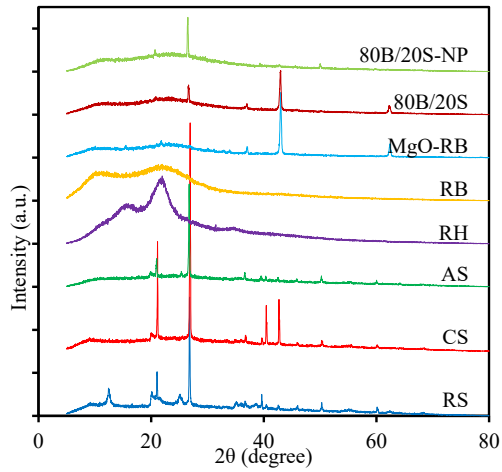

Figure 8: XRD results of raw rice husk (RH), rice husk biochar (RB), MgO-modified rice husk biochar (MgO-RB), 80B/20S composite before (80B/20S) and after (80B/20S-NP) adsorption, raw alum sludge (RS), calcined alum sludge (CS), and acid-activated alum sludge (AS).

3.3 *Characterization of the materials*

Figure 8 plots the XRD patterns of the prepared materials. Raw rice husk (RH) and rice husk biochar (RB) show diffraction peaks at 2θ of 15° and 22°, which are characteristic peaks of amorphous silicon. For MgO-modified rice husk biochar (MgO-RB), obvious characteristic peaks of crystalline MgO particles are observed at 2θ of 37, 43, and 62.5°, which is consistent with other reports in the literature [5], [11], [50]. According to XRD data, the initial raw sludge material (RS) contains 70.7% amorphous components with the rest of 29.3% existing in the form of crystals, including peaks at 2θ of 21.5, 27, 37, 39.5,

Table 3: Results of actual domestic wastewater treatment

Sample	Initial Concentration (mg/L)		Adsorption Capacity (mg/g)		Removal Efficiency (%)	
	NH_4^+	PO_4^{3-}	NH_4^+	PO_4^{3-}	NH_4^+	PO_4^{3-}
WW1	68.85	19.59	63.64±1.09	16.53±0.10	93.71±1.14	85.57±1.05
WW2	20.40	2.62	19.77±0.29	2.58±0.02	98.28±1.08	100±0.00

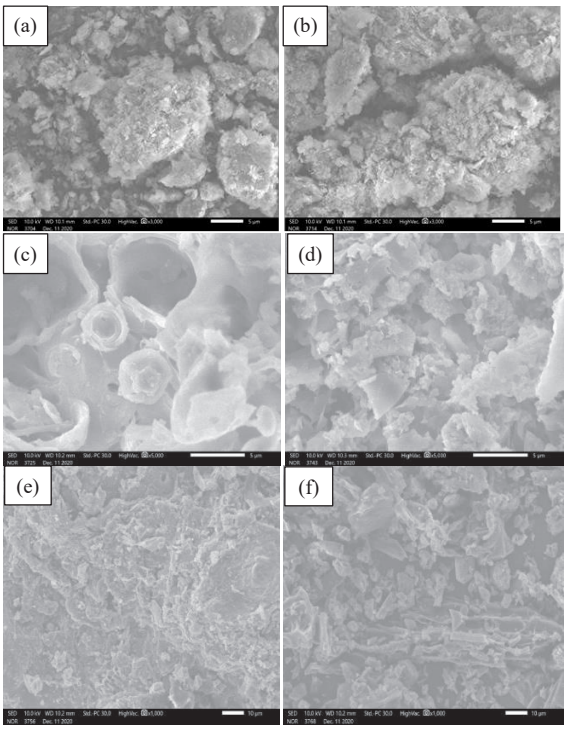

Figure 9: SEM images of raw alum sludge (a), activated alum sludge (b), raw rice husk (c), MgO-modified rice husk biochar (d), and 80B/20S composite before (e) and after (f) adsorption.

43, 46, 50.5, and 60 of SiO_2 crystals and 12.5, 20, and 25° of MnO. After being calcined at 500 ℃ (CS) within 1 h, the peak intensity of SiO_2 crystal increased, resulting in crystal phase composition increased to 31.4%. After being activated with H_2SO_4 (AS), the peak intensity of SiO_2 was reduced and the percentage of crystals was only 18.4%. This is because when the sludge is activated with the acid, the acid treatment converted the crystal structure of silicon from its stable to amorphous form.

XRD pattern of 80B/20S before adsorption (80B/20S) has characteristic components such as MgO in biochar and SiO_2 in sludge (Figure 9). The characteristic peaks of MgO are observed at 2θ of 37, 43, and 62.5°, which are like MgO-RB material, and the characteristic peaks of SiO_2 are observed at 2θ of 21 and 27°, which are like AS material. This partly proves that the mixed material has homogeneity, and the composite has characteristics of both components. After the ammonium and phosphate adsorption, the 80B/20S composite had a clear change in the composition of compounds that were present in the material structure. MgO particles on the surface of the 80B/20S material, before being adsorbed, participate in reactions, and form chemical bonds with ammonium and phosphate ions to form complexes or precipitates in 80B/20S-NP material. This was evidenced by the intensity reduction of the MgO crystal characteristic peaks at 2θ of 37, 43, and 62.5° and the appearance of new peaks at 2θ of 39.5, 46, 50.5, and 60°, which were typical for struvite crystal ($NH_4MgPO_4.6H_2O$). The value of MgO particles on the surface of the material, as well as the application of the post-adsorption material as a slow-release fertilizer due to its struvite content, were revealed by the XRD analysis results of the material before and after adsorption.

Figure 9 shows the SEM morphology of the materials, while Table 4 summarizes the surface elemental composition of the materials. Regarding alum sludge, SEM images in Figure 9(a) and (b) show that there was not much difference between the raw and the acid-activated alum sludge. However, activated sludge had more uniformity of porous structure distribution because of the loss of some impurities as well as organic matter after the heat and acid treatment. This was also reflected in the carbon content in the raw sludge material (14.28 ± 0.08%), which sharply decreased to 2.78 ± 0.04% in the activated sludge due (Table 4). Besides, rice husk composes mainly of organic compounds, so there was a clear change in material structure as well as surface morphology before and after MgO impregnation and heat treatment. As observed from Figure 9(c) and (d), the surface structure of the rice husk greatly changed after modification. Raw rice husks had a large hollow structure and a smooth surface, while modified rice husks had a more porous structure. Also, the material's surface is covered with MgO particles leads to form many small sponges and relatively porous structures. The carbonization and MgO impregnation increased the carbon content, reduced the oxygen content, and introduced Mg and Cl contents to the modified rice husk biochar (Table 4). These results indicated that MgO particles were successfully impregnated on the surface of rice husk biochar, which significantly enhances the porous structure of the material and facilitates the adsorption of ammonium and phosphate.

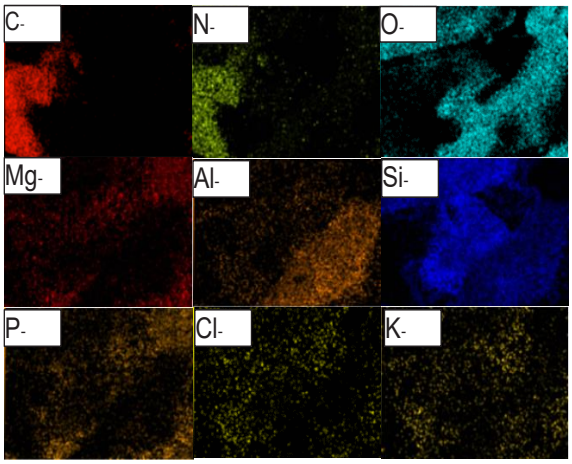

Figure 10: EDX-mapping results of 80B/20S composite after ammonium and phosphate adsorption.

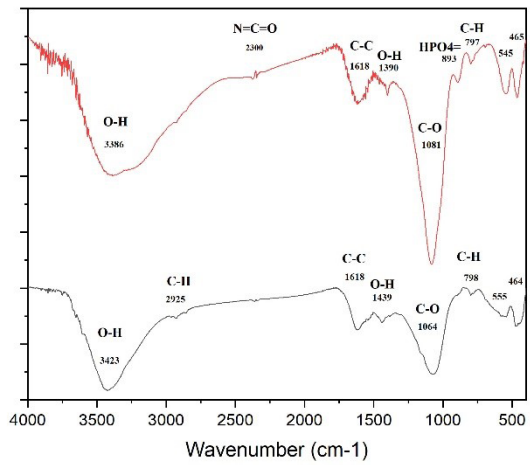

Figure 11: FTIR spectra 80B/20S composite before (80B/20S) and after (80B/20S-NP) adsorption.

EDX results in Table 4 show that the constituents of the 80B/20S material before adsorption mainly contain characteristic elements of biochar and sludge such as C, O, Si, Mg, Cl, and K. After adsorption, there are N and P elements on the surface of the 80B/20S-NP material, proving the successful adsorption of N and P on the surface of the 80B/20S material. The removal of N and P from water through the adsorption mechanism was also proven through the distribution of elements in the 80B/20S composite after ammonium and phosphate adsorption by the EDX-mapping method, as shown in Figure 10. The phosphorous element is distributed evenly on the surface of the material with a mass ratio of 3.42 % while the nitrogen element accounts for 1.15% of the total mass of the elements constituting the material. These results proved that biochar combined with sludge material has a good ability to adsorb ammonium and phosphate ions from water.

Infrared spectroscopy is useful for identifying functional groups on a material's surface and characterizing the material's surface chemical properties. Figure 11 presents the FTIR spectra of 80B/20S composite before and after the adsorption to partly clarify the ammonium and phosphate removal mechanism of this material. Both the composite before and after adsorption had diffraction peaks at positions ranging from 3386–3423 cm^{-1}, 1618 cm^{-1}, 1390–1439 cm^{-1}, 1064–1081 cm^{-1}, and 797–798 cm^{-1}, which are characterized for organic bonds such as O-H, C-C,

Table 4: Compositions and content of elements in raw sludge (RS) and acid activated sludge (AS), raw (RH) and modified rice husk (MgO-RB), 80B/20S and 80B/20S-NP

Elements	Mass (%)					
	RS	AS	RH	MgO-RB	80B/20S	80B/20S-NP
C	14.28±0.08	2.78±0.04	46.90±0.09	50.17±0.11	27.51±0.09	29.63±0.08
O	52.14±0.18	57.25±0.16	49.23±0.17	24.36±0.12	36.10±0.14	40.80±0.12
Al	14.71±0.12	15.38±0.11	0.24±0.02	-	0.38±0.02	4.33±0.04
Si	18.07±0.14	21.86±0.14	3.35±0.05	0.84±0.03	2.22±0.05	16.54±0.09
K	0.80±0.06	0.74±0.05	0.28±0.03	0.18±0.03	0.38±0.04	0.32±0.03
S	-	1.98±0.05	-	-	-	-
Mg	-	-	-	16.88±0.08	27.73±0.13	3.37±0.04
Cl	-	-	-	7.58±0.08	5.32±0.08	0.44±0.02
N	-	-	-	-	-	1.15±0.03
P	-	-	-	-	-	3.42±0.05

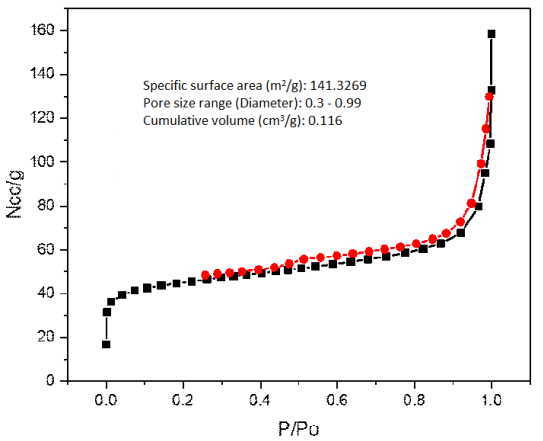

Figure 12: The N_2 adsorption-desorption isotherms of 80B/20S composite.

C-O, and C-H. The results of Zhang *et al.*, found that the disappearance of some groups such as C=O and C=C demonstrated the reaction between them with ammonium removal [51]. According to some studies, the presence of these functional groups on the material surface played a significant role in removing ions from the solution through the ion exchange mechanism and electrostatic attraction [12], [41]. The related groups appeared after adsorption, with peaks at 2300 cm^{-1} and 893 cm^{-1}, respectively, which are characteristic peaks of the functional groups N=C=O and HPO_4=, demonstrating the effective adsorption of ammonium and phosphate on the surface of the 80B/20S composite.

The specific surface area is an important parameter to evaluate the porous structure of an adsorbent. The N_2 adsorption isotherm and the specific surface area of the 80B/20S composite are shown in Figure 12. The adsorption isotherms can be classified into Type II of the adsorption isotherms for the materials with have both high surface area for monolayer adsorption and pore structure for capillary condensation. The hysteresis of the adsorption-desorption curve belongs to Type A of the pore systems which is similar to cylindrical pores with opened ends. The specific surface area of the 80B/20S material measured by the BET method was 141.3269 m^2/g, which was much higher than some other biochar materials, such as acacia (3.57 m^2/g), vetiver (83.01 m^2/g), reed (107.82 m^2/g) modified at the same temperature of 500 °C [41], biochar from pineapple modified with $La(OH)_3$ (84.89 m^2/g) [52], and MgFe-LDH modified biochar (3.9 m^2/g) [53]. This high specific surface area was thought to be a key factor in the 80B/20S composite's high adsorption potential for ammonium and phosphate removal.

4 Conclusions

The biochar-sludge composite of MgO-modified rice husk and acid sludge was successfully synthesized and applied for the recovery of ammonium and phosphate in wastewater. The properties of composite material (MgO rice husk and H_2SO_4 sludge) were analyzed through modern techniques, such as X-ray diffraction, FTIR, EDX, and BET. The optimum conditions for the fabrication of rice husk material were found at $MgCl_2$ content of 4%, 500 °C for 15 min while alum sludge should be activated by annealing at 500 °C and followed by sulfuric acid treatment. The most feasible ratio for high ammonium and phosphate adsorption potential was a mixture of 80% adjusted biochar and 20% activated sludge. At 200 mg/L inlet concentration and 8 h of adsorption, the adsorption capacity of the composite was getting saturated. The adsorption of ammonium and phosphate was best characterized by the Langmuir isotherm model, with maximum adsorption capacities of 185.53 mgNH_4^+/g and 63.78 mgPO_4^{3-}/g, respectively. For the actual wastewater, the removal efficiency of phosphate and ammonium ion was both above 85%. These findings point to a promising strategy for using rice husk and alum sludge as an effective composite for recovering nitrogen and phosphorus from wastewater and using the nutritious composite as a source of slow-release fertilizer for sustainable agriculture after adsorption. In the future, more composite material with other biomasses and sludges, different wastewaters, and other modification methods might be concerned for more information.

Acknowledgments

We acknowledge Ho Chi Minh City University of Technology (HCMUT), VNU-HCM for supporting this study.

Author Contributions

N.T.V.A: formal analysis, investigation, data curation,

writing - original draft preparation, visualization; N.N.H.: formal analysis, investigation, supervision, project administration, funding acquisition; N.T.T.: conceptualization, methodology, data curation, writing - original draft preparation, supervision, project administration; N.L.T.: writing - review and editing, visualization; N.N.H.: conceptualization, methodology, writing - review and editing, project administration, funding acquisition. All authors have read and agreed to the published version of the manuscript.

Conflicts of Interest

The authors declare no conflict of interest.

References

[1] Q. Yin, M. Liu, and H. Ren, "Removal of ammonium and phosphate from water by Mg-modified biochar: Influence of Mg pretreatment and pyrolysis temperature," *BioResources*, vol. 14, pp. 6203–6218, 2019.

[2] H. Zhang, R. Voroney, and G. Price, "Effects of temperature and activation on biochar chemical properties and their impact on ammonium, nitrate, and phosphate sorption," *Journal of Environmental Quality*, vol. 46, pp. 889–896, 2017.

[3] P. T. Phan, T. T. Nguyen, N. H. Nguyen, and S. Padungthon, "Triamine-bearing activated rice husk ash as an advanced functional material for nitrate removal from aqueous solution," *Water Science and Technology*, vol. 79, pp. 850–856, 2019.

[4] Y. Yao, B. Gao, M. Inyang, A. R. Zimmerman, X. Cao, P. Pullammanappallil, and L. Yang, "Removal of phosphate from aqueous solution by biochar derived from anaerobically digested sugar beet tailings," *Journal of Hazardous Materials*, vol. 190, pp. 501–507, 2011.

[5] M. Zhang, B. Gao, Y. Yao, Y. Xue, and M. Inyang, "Synthesis of porous MgO-biochar nanocomposites for removal of phosphate and nitrate from aqueous solutions," *Chemical Engineering Journal*, vol. 210, pp. 26–32, 2012.

[6] Z. Wang, H. Guo, F. Shen, G. Yang, Y. Zhang, Y. Zeng, L. Wang, H. Xiao, and S. Deng, "Biochar produced from oak sawdust by Lanthanum (La)-involved pyrolysis for adsorption of ammonium (NH_4^+), nitrate (NO_3^-), and phosphate (PO_4^{3-})," *Chemosphere*, vol. 119, pp. 646–653, 2015.

[7] S. Wan, S. Wang, Y. Li, and B. Gao, "Functionalizing biochar with Mg–Al and Mg–Fe layered double hydroxides for removal of phosphate from aqueous solutions," *Journal of Industrial and Engineering Chemistry*, vol. 47, pp. 246–253, 2017.

[8] T. Sizmur, T. Fresno, G. Akgül, H. Frost, and E. Moreno-Jiménez, "Biochar modification to enhance sorption of inorganics from water," *Bioresource Technology*, vol. 246, pp. 34–47, 2017.

[9] L. He, D. Wang, Z. Wu, Y. Lv, and S. Li, "Magnesium-modified biochar was used to adsorb phosphorus from wastewater and used as a phosphorus source to be recycled to reduce the ammonia nitrogen of piggery digestive wastewater," *Journal of Cleaner Production*, vol. 360, 2022, Art. no. 132130.

[10] R. Xiao, H. Zhang, Z. Tu, R. Li, S. Li, Z. Xu, and Z. Zhang, "Enhanced removal of phosphate and ammonium by MgO-biochar composites with NH(3)·H(2)O hydrolysis pretreatment," Environmental Science and Pollution Research, vol. 27, pp. 7493–7503, 2020.

[11] R. Li, J. J. Wang, B. Zhou, Z. Zhang, S. Liu, S. Lei, and R. Xiao, "Simultaneous capture removal of phosphate, ammonium and organic substances by MgO impregnated biochar and its potential use in swine wastewater treatment," *Journal of Cleaner Production*, vol. 147, pp. 96–107, 2017.

[12] C. C. Hollister, J. J. Bisogni, and J. Lehmann, "Ammonium, nitrate, and phosphate sorption to and solute leaching from biochars prepared from corn stover (*Zea mays* L.) and oak wood (*Quercus* spp.)," *Journal of Environmental Quality*, vol. 42, pp. 137–144, 2013.

[13] Y. Yao, B. Gao, M. Inyang, A. R. Zimmerman, X. Cao, P. Pullammanappallil, and L. Yang, "Biochar derived from anaerobically digested sugar beet tailings: Characterization and phosphate removal potential," *Bioresource Technology*, vol. 102, pp. 6273–6278, 2011.

[14] D. Jiang, B. Chu, Y. Amano, and M. Machida, "Removal and recovery of phosphate from water by Mg-laden biochar: Batch and column studies," *Colloids and Surfaces A: Physicochemical and Engineering Aspects*, vol. 558, pp. 429–437, 2018.

[15] K. Butterbach-Bahl, D. Kraus, R. Kiese, V. T. Mai, T. Nguyen, B. O. Sander, R. Wassmann, and C. Werner, "Activity data on crop management define uncertainty of CH4 and N_2O emission estimates from rice: A case study of Vietnam," *Journal of Plant Nutrition and Soil Science*, vol. 185, pp. 793–806, 2022.

[16] M. Keck and D. T. Hung, "Burn or bury? A comparative cost–benefit analysis of crop residue management practices among smallholder rice farmers in northern Vietnam," *Sustainability Science*, vol. 14, pp. 375–389, 2018.

[17] P. T. Duong and H. Yoshiro, "Current situation and possibilities of rice straw management in Vietnam," *University of Tsukuba, Ibaraki, Japan*, 2015.

[18] N. T. T. Truc, Z. M. Sumalde, M. V. O. Espaldon, E. P. Pacardo, C. L. Rapera, and F. G. Palis, "Farmers' awareness and factors affecting adoption of rapid composting in Mekong Delta, Vietnam and Central Luzon, Philippines," *Journal of Environmental Science Management and Compliance Series*, vol. 15, no. 2, pp. 59–73, 2012.

[19] SNV, "Biomass business opportunities in Vietnam," 2012. [Online]. Available: http://www.snvworld.org/en/vietnam/publications/biomass-business-opportunities-in-vietnam

[20] T. Q. Cong and D. N. Hien, "Feasibility of cleaner production for vietnam rice processing industry," *Procedia CIRP*, vol. 40, pp. 285–288, 2016.

[21] B. Bushra and N. Remya, "Biochar from pyrolysis of rice husk biomass—characteristics, modification and environmental application," *Biomass Conversion and Biorefinery*, 2020.

[22] K. Simon, W. Shubiao, W, L. Ming, L. Qimin, B. Hamidou, and D. Renjie, "Evaluation of slow pyrolyzed wood and rice husks biochar for adsorption of ammonium nitrogen from piggery manure anaerobic digestate slurry," *Science of the Total Environment*, vol. 505, pp. 102–112, 2015.

[23] K. Herrera, L. F. Morales, N. A. Tarazona, R. Aguado, and J. F. Saldarriaga, "Use of biochar from rice husk pyrolysis: Part A: Recovery as an adsorbent in the removal of emerging compounds," *ACS Omega*, vol. 7, pp. 7625–7637, Mar. 2022.

[24] A. A. H. Saeed, N. Y. Harun, M. M. Nasef, A. Al-Fakih, A. A. S. Ghaleb, and H. K. Afolabi, "Removal of cadmium from aqueous solution by optimized rice husk biochar using response surface methodology," *Ain Shams Engineering Journal*, vol. 13, vol. 13, no. 1, 2022, Art. no. 101516.

[25] Q. Yin, B. Zhang, R. Wang, and Z. Zhao, "Biochar as an adsorbent for inorganic nitrogen and phosphorus removal from water: A review," *Environmental Science and Pollution Research*, vol. 24, pp. 26297–26309, 2017.

[26] R. Singh and M. Agrawal, "Potential benefits and risks of land application of sewage sludge," *Waste Management*, vol. 28, pp. 347–358, 2008.

[27] Y. Yang, Y. Zhao, A. Babatunde, L. Wang, Y. Ren, and Y. Han, "Characteristics and mechanisms of phosphate adsorption on dewatered alum sludge," *Separation and Purification Technology*, vol. 51, pp. 193–200, 2006.

[28] A. Babatunde, Y. Yang, and Y. Zhao, "Towards the development of a novel wastewater treatment system incorporating drinking water residual: Preliminary results," in *10th European Biosolids Conference*, 2005.

[29] J. G. Kim, J. H. Kim, H.-S. Moon, C.-M. Chon, and J. S. Ahn, "Removal capacity of water plant alum sludge for phosphorus in aqueous solutions," *Chemical Speciation & Bioavailability*, vol. 14, pp. 67–73, 2002.

[30] A. Babatunde and Y. Zhao, "Equilibrium and kinetic analysis of phosphorus adsorption from aqueous solution using waste alum sludge," *Journal of Hazardous Materials*, vol. 184, pp. 746–752, 2010.

[31] M. Kończak and M. Huber, "Application of the engineered sewage sludge-derived biochar to minimize water eutrophication by removal of ammonium and phosphate ions from water," *Journal of Cleaner Production*, vol. 331, 2022, Art. no. 129994.

[32] Q. He, X. Li, and Y. Ren, "Analysis of the

simultaneous adsorption mechanism of ammonium and phosphate on magnesium-modified biochar and the slow release effect of fertiliser," *Biochar*, vol. 4, 2022, Art. no. 25.

[33] Y. H. Jiang, A. Y. Li, H. Deng, C. H. Ye, Y. Q. Wu, Y. D. Linmu, and H. L. Hang, "Characteristics of nitrogen and phosphorus adsorption by Mg-loaded biochar from different feedstocks," *Bioresource Technology*, vol. 276, pp. 183–189, 2019.

[34] C. A. Takaya, L. A. Fletcher, S. Singh, K. U. Anyikude, and A. B. Ross, "Phosphate and ammonium sorption capacity of biochar and hydrochar from different wastes," *Chemosphere*, vol. 145, pp. 518–527, 2016.

[35] G. A. Adebisi, Z. Z. Chowdhury, and P. A. Alaba, "Equilibrium, kinetic, and thermodynamic studies of lead ion and zinc ion adsorption from aqueous solution onto activated carbon prepared from palm oil mill effluent," *Journal of Cleaner Production*, vol. 148, pp. 958–968, 2017.

[36] Y. Zhao, Y. Yang, S. Yang, Q. Wang, C. Feng, and Z. Zhang, "Adsorption of high ammonium nitrogen from wastewater using a novel ceramic adsorbent and the evaluation of the ammonium-adsorbed-ceramic as fertilizer," *Journal of Colloid and Interface Science*, vol. 393, pp. 264–270, 2013.

[37] G. Peng, S. Jiang, Y. Wang, Q. Zhang, Y. Cao, Y. Sun, W. Zhang, and L. Wang, "Synthesis of Mn/Al double oxygen biochar from dewatered sludge for enhancing phosphate removal," *Journal of Cleaner Production*, vol. 251, 2020, Art. no. 119725.

[38] R. Li, J. J. Wang, B. Zhou, M. K. Awasthi, A. Ali, Z. Zhang, L. A. Gaston, A. H. Lahori, and A. Mahar, "Enhancing phosphate adsorption by Mg/Al layered double hydroxide functionalized biochar with different Mg/Al ratios," *The Science of the Total Environment*, vol. 559, pp. 121–129, 2016.

[39] Z. Danchen, Y. Haiping, C. Xu, C. Wei, C. Ning, C. Yingquan, Z. Shihong, and C. Hanping, "Temperature-dependent magnesium citrate modified formation of MgO nanoparticles biochar composites with efficient phosphate removal," *Chemosphere*, vol. 274, 2021, Art. no. 129904.

[40] M. M. T. Zin and D. J. Kim, "Simultaneous recovery of phosphorus and nitrogen from sewage sludge ash and food wastewater as struvite by Mg-biochar," *Journal of Hazardous Materials*, vol. 403, 2021, Art. no. 123704.

[41] Z. Zeng, T.-q. Li, F.-l. Zhao, Z.-l. He, H.-p. Zhao, X.-e. Yang, H.-l. Wang, J. Zhao, and M. T. Rafiq, "Sorption of ammonium and phosphate from aqueous solution by biochar derived from phytoremediation plants," *Journal of Zhejiang University Science B*, vol. 14, pp. 1152–1161, 2013.

[42] D. Luo, L. Wang, H. Nan, Y. Cao, H. Wang, T. V. Kumar, and C. Wang, "Phosphorus adsorption by functionalized biochar: A review," *Environmental Chemistry* Letters, vol. 21, pp. 497–524, 2022.

[43] L. Dai, B. Wu, F. Tan, M. He, W. Wang, H. Qin, X. Tang, Q. Zhu, K. Pan, and Q. Hu, "Engineered hydrochar composites for phosphorus removal/recovery: Lanthanum doped hydrochar prepared by hydrothermal carbonization of lanthanum pretreated rice straw," *Bioresource Technology* vol. 161, pp. 327–332, 2014.

[44] H. Liu, Y. Dong, H. Wang, and Y. Liu, "Ammonium adsorption from aqueous solutions by strawberry leaf powder: Equilibrium, kinetics and effects of coexisting ions," *Desalination*, vol. 263, pp. 70–75, 2010.

[45] Z. Wang, D. Shen, F. Shen, and T. Li, "Phosphate adsorption on lanthanum loaded biochar," *Chemosphere*, vol. 150, pp. 1–7, 2016.

[46] N. Cheng, B. Wang, Q. Feng, X. Zhang, and M. Chen, "Co-adsorption performance and mechanism of nitrogen and phosphorus onto eupatorium adenophorum biochar in water," *Bioresource Technology*, vol. 340, 2021, Art. no. 125696.

[47] H. Cruz, P. Luckman, T. Seviour, W. Verstraete, B. Laycock, and I. Pikaar, "Rapid removal of ammonium from domestic wastewater using polymer hydrogels," *Scientific Reports*, vol. 8, pp. 1–6, 2018.

[48] J. Pesonen, P. Myllymäki, S. Tuomikoski, G. Vervecken, T. Hu, H. Prokkola, P. Tynjälä, and U. Lassi, "Use of calcined dolomite as chemical precipitant in the simultaneous removal of ammonium and phosphate from synthetic

wastewater and from agricultural sludge," *ChemEngineering*, vol. 3, 2019, Art. no. 40.

[49] B. Wu, L. Fang, J. D. Fortner, X. Guan, and I. M. Lo, "Highly efficient and selective phosphate removal from wastewater by magnetically recoverable $La(OH)_3/Fe_3O_4$ nanocomposites," *Water Research*, vol. 126, pp. 179–188, 2017.

[50] Q. Yin, R. Wang, and Z. Zhao, "Application of Mg–Al-modified biochar for simultaneous removal of ammonium, nitrate, and phosphate from eutrophic water," *Journal of Cleaner Production*, vol. 176, pp. 230–240, 2018.

[51] Z. Ming, G. Bin, Y. Ying, and I. Mandu, "Phosphate removal ability of biochar/MgAl-LDH ultra-fine composites prepared by liquid-phase deposition," *Chemosphere*, vol. 92, pp. 1042–1047, 2013.

[52] T. Li, X. Su, X. Yu, H. Song, Y. Zhu, and Y. Zhang, "$La(OH)_3$-modified magnetic pineapple biochar as novel adsorbents for efficient phosphate removal," *Bioresource Technology*, vol. 263, pp. 207–213, 2018.

[53] L. Xue, B. Gao, Y. Wan, J. Fang, S. Wang, Y. Li, R. Muñoz-Carpena, and L. Yang, "High efficiency and selectivity of MgFe-LDH modified wheat-straw biochar in the removal of nitrate from aqueous solutions," *Journal of the Taiwan Institute of Chemical Engineers*, vol. 63, pp. 312–317, 2016.